Received: 9 April 2020 | Revised: 11 August 2020 | Accepted: 12 August 2020

DOI: 10.1111/epi.16680

FULL-LENGTH ORIGINAL RESEARCH

Epilepsia®

Preictal variability of high-frequency oscillation rates in refractory epilepsy

Jared M. Scott[1] | **Sijin Ren**[2] | **Stephen V. Gliske**[1,3] | **William C. Stacey**[1,2,3,4]

[1]Department of Biomedical Engineering, University of Michigan, Ann Arbor, Michigan

[2]Neuroscience Graduate Program, University of Michigan, Ann Arbor, Michigan

[3]Department of Neurology, University of Michigan, Ann Arbor, Michigan

[4]Biointerfaces Institute, University of Michigan, Ann Arbor, Michigan

Correspondence
William C. Stacey, Department of Neurology and Department of Biomedical Engineering, University of Michigan, 1500 E Medical Center Dr, SPC 5036, Ann Arbor, MI 48109.
Email: William.stacey@umich.edu

Funding information
University of Michigan Medical School, Grant/Award Number: Lucas Family Research Fund, and Robbins Family Research Fund; National Institutes of Health, Grant/Award Number: K01-ES026839, and R01-NS094399

Abstract

Objective: High-frequency oscillations (HFOs) have shown promising utility in the spatial localization of the seizure onset zone for patients with focal refractory epilepsy. Comparatively few studies have addressed potential temporal variations in HFOs, or their role in the preictal period. Here, we introduce a novel evaluation of the instantaneous HFO rate through interictal and peri-ictal epochs to assess their usefulness in identifying imminent seizure onset.

Methods: Utilizing an automated HFO detector, we analyzed intracranial electroencephalographic data from 30 patients with refractory epilepsy undergoing long-term presurgical evaluation. We evaluated HFO rates both as a 30-minute average and as a continuous function of time and used nonparametric statistical methods to compare individual and population-level differences in rate during peri-ictal and interictal periods.

Results: Mean HFO rate was significantly higher for all epochs in seizure onset zone channels versus other channels. Across the 30 patients of our cohort, we found no statistically significant differences in mean HFO rate during preictal and interictal epochs. For continuous HFO rates in seizure onset zone channels, however, we found significant population-wide increases in preictal trends relative to interictal periods. Using a data-driven analysis, we identified a subset of 11 patients in whom either preictal HFO rates or their continuous trends were significantly increased relative to those of interictal baseline and the rest of the population.

Significance: These results corroborate existing findings that HFO rates within epileptic tissue are higher during interictal periods. We show this finding is also present in preictal, ictal, and postictal data, and identify a novel biomarker of preictal state: an upward trend in HFO rate leading into seizures in some patients. Overall, our findings provide preliminary evidence that HFOs can function as a temporal biomarker of seizure onset.

KEYWORDS
high-frequency oscillation, preictal biomarker, seizure prediction, temporal biomarker

1 | INTRODUCTION

High-frequency oscillations (HFOs) have shown promise in clinical epilepsy research as a biomarker of epileptic tissue. Defined as short bursts of neural activity > 80 Hz, HFOs occur more frequently in epileptic tissue.[1,2] Numerous studies have shown that HFOs accurately delineate the seizure onset zone and potentially improve surgical outcomes.[3–7] Although most HFO studies concentrate on localization of abnormal channels, there is interest in characterizing other aspects of HFOs and epilepsy.[8] As high-frequency activity has been shown to increase prior to seizure onset both clinically and in experimental models,[9–11] some have also hypothesized a link between HFOs, the mechanisms of ictogenesis, and preictal brain states.[10–18]

The existence of a preictal state is still unproven, but growing evidence suggests it is measurable in many patients.[19–21] One notable study found differences in preictal electroencephalogram (EEG) occurring even hours before seizure onset.[20] However, very few studies address HFOs in the preictal period. Early work with small cohorts showed that preictal HFOs have subtle changes in the preictal period, such as spectral and rate changes[22] or alterations in HFO features.[23] Newer hardware and software now make HFO research much more robust, allowing high-quality, larger datasets[13,23–27]; the role of HFOs as a preictal biomarker can now be answered with much higher rigor. To our knowledge, there is no study of peri-ictal HFO rates using modern equipment and algorithms to acquire a robust sample size. This has halted further progress toward our understanding of the temporal evolution of HFOs and their relationship to mechanisms of seizure generation and termination. Furthermore, it has prevented the adoption of HFOs as a temporal biomarker.

We designed this study to directly address these deficits. Here, we analyze >11 million automatically detected HFOs from the entire intracranial EEG record of 30 patients. We adapt the analysis to generate the first robust comparison of peri- and interictal HFO rates. We find a subset of patients in whom HFO rates change up to 30 minutes prior to seizures, which we suggest can be used as a temporal biomarker of impending seizure onset in future seizure prediction applications.

Key Points

- Mean HFO rate increases preictally in a subset of patients
- cHFO rate estimates rate as a function of time
- Preictal cHFO rates have an upward slope in a subset of patients
- HFOs have potential as a temporal biomarker of seizure onset

2 | MATERIALS AND METHODS

2.1 | Patient population

Data were acquired from all consecutive patients at the University of Michigan who had intracranial EEG (iEEG) monitoring for refractory epilepsy with at least 4096 Hz sampling rate from 2016 to 2018. For inclusion in the study, patients had to have a total recorded time of at least 24 hours, during which at least 1 seizure occurred. Additionally, we required sufficient metadata regarding channel mappings, seizure times, and other clinical data. This produced a total of 30 patients for the study. Electrodes implanted for monitoring included a mix of subdural grids, conventional depth electrodes, and stereo-EEG electrodes. Channels were labeled as "seizure onset zone," and seizure onset/offset times were determined, according to the official clinical report of the treating epileptologist. Channels were labeled as lying within "resected volume" by consultation with the neurosurgeon and comparison of pre- and postoperative imaging (when available). Prior to data acquisition, full institutional review board approval was obtained, as well as written consent from patients to share their deidentified data. All EEG data were acquired with a Quantum amplifier (Natus Medical) with a sampling rate of 4096 Hz. Further summary of the patient population can be found in Table 1.

2.2 | Data processing and analysis

All data were analyzed using custom C++ and MATLAB (MathWorks) packages and scripts. As seen in Figure 1, our data analysis workflow consisted of three main components: automated HFO detection, indexing and windowing operations, and statistical analysis of mean and continuous HFO rates. These individual steps are described below.

2.3 | Automatic HFO detection and electromyographic artifact removal

For automated HFO detection, we used a previously validated HFO detector.[27] Briefly summarized, we use the highly sensitive "Staba" detector[28] on band-passed (80-500 Hz) data, then redact detections likely to be due to artifacts, leaving more specific "quality HFOs" (qHFOs). We also applied an additional, published artifact rejection method designed to redact activity associated with scalp muscle artifact, which can produce many false-positive detections in the lateral

temporal lobes.[26] All HFOs discussed in this work were subjected to this full process.

2.4 | Adjusting HFO detector for peri-ictal periods

All resulting HFOs for a given patient were labeled as either interictal baseline or peri-ictal, which we defined to include the full period from 30 minutes prior to 30 minutes after a seizure. Interictal HFOs were indexed into a successive series of interictal windows whose individual duration was 30 minutes. Peri-ictal detections were further subdivided into three continuous epochs: preictal, ictal, and postictal. We defined the preictal and postictal epochs as beginning 30 minutes before and ending 30 minutes after the ictal epoch, respectively. The ictal epoch was defined by the clinical mark of beginning and end, as well as an additional 1-minute buffer before and after the seizure. This buffer was added to mitigate potential inconsistencies in clinically marked seizure times, which can vary between clinicians.[29,30] A schematic showing the exact timing of these epochs is given in Figure 1C.

Most automated HFO detectors are designed for interictal data, where the EEG baseline is assumed to be relatively stable over time; the HFO detection algorithm compares with the baseline EEG every 10 minutes, which is assumed to be interictal.[28] However, including peri-ictal data presents a new challenge, because a seizure changes the "baseline" significantly and disrupts the threshold for HFO detection. To address these considerations, we used two simple modifications to our HFO detection process during peri-ictal periods.

The first modification was designed to align the 10-minute windows correctly to ensure ictal data were not present in the preictal epochs. This did not change the method of HFO detection, merely the start and stop times for the preictal epochs. During peri-ictal periods, the baseline was referenced to the start of the seizure, that is, the HFO detector was started 31 minutes prior to each seizure onset, which includes the aforementioned 1-minute buffer. From this point, the detector ran in successive 10-minute segments until reaching the end of the postictal epoch as we have defined it above. Aligning the qHFO detector in this manner ensured that ictal EEG activity did not contaminate the preictal baseline threshold used to identify HFOs. Note that if baseline also increased preictally, this would lead to fewer HFOs being detected during the preictal period. Thus, the results herein are a conservative estimate of preictal HFOs.

Second, we fixed the "baseline" threshold used for ictal and postictal HFO detection to the value of the 10-minute preictal segment just prior to the ictal period. This ensured that ictal and postictal rates were scaled to preictal baseline, rather than ictal activity. This was necessary because ictal data typically have a much higher baseline root mean square value than the preictal portion that precedes it, and our understanding of "increased HFO rates," as well as the automated detector, is based upon comparison with interictal baseline. This method ensured the ictal and postictal rates would be referenced to the preictal baseline, prior to any ictal activity.

2.5 | Window exclusion and alignment

Because the peri-ictal and interictal data have different reference points, it is possible that the windows overlap with each other or with periods of unreliable data. To ensure data quality and no overlap, we excluded windows that could be unreliable (Figure 1B). Specifically, we redacted windows that had overlap with any of the following conditions: (1) any other window, (2) file start or stop times, (3) gaps in recorded data of 1 minute or more, and (4) known extraoperative mapping procedures or other similar periods of poor data quality. Windows meeting any of these conditions were labeled unusable and excluded from further analysis. After this procedure, there were 217 seizures available for processing in the 30 patients. Remaining windows were then sorted according to type (ie, interictal baseline or peri-ictal) and aligned in time, which allowed comparison of HFO times across all windows. Grouping these windows then allowed computation of average HFO rates as described below.

2.6 | Computing HFO rate

Our analysis utilized two different representations of HFO rate: mean HFO rate and continuous HFO (cHFO) rate. These values were computed across two groups of intracranial channels: seizure onset zone channels (hereafter abbreviated SOZ), and all channels that were outside of both the SOZ and the volume of resected tissue (RV), which we denote OUT. Note that there is usually a great deal of overlap between SOZ and RV, but RV often has many channels that were not in the SOZ, and may not contain all of the SOZ, depending upon clinical circumstances. Mean HFO rate was computed as the average over all usable windows and was defined as the total number of HFOs divided by the product of the number of channels and total duration of the windows used.

2.7 | cHFO rate: The Nelson-Aalen hazard rate

A robust analysis of temporal characteristics of HFOs requires information on their rate as a function of time, rather

TABLE 1 Clinical data

Subject	Age, y	Sex	ILAE outcome	Seizure focus, hemisphere/ region	Pathology/*implant type*	Intracranial channels, n			
						Total	ECoG	Depth	SOZ
UMHS-0019	59	F	II	R/T	Gliosis	106	106	0	2
UMHS-0020	45	F	II	R/T	MTS	25	0	25	9
UMHS-0021	30	M	II	R/T	Gliosis, PVNH, PMG	46	0	46	13
UMHS-0022	40	M	I	L/T	CD, MTS	38	0	38	3
UMHS-0023	29	M	NR	L/T, P	PVNH/*Neuropace*	69	41	28	29
UMHS-0024	31	M	NR	L, R/T	*Neuropace*	75	55	20	16
UMHS-0025	17	F	II	L/T	Gliosis	20	0	20	5
UMHS-0026	22	F	NR	R/T	PVNH	52	0	52	3
UMHS-0027	26	M	NR	L/diffuse	*VNS*	91	81	10	3
UMHS-0028	14	F	I	R/T	Tumor: glioma	53	47	6	5
UMHS-0029	48	M	NR	L/T, Occ	*Neuropace*	91	91	0	22
UMHS-0030	5	M	III	L/T	MTS, gliosis	100	100	0	2
UMHS-0031	13	M	I	L/T	Gliosis, tumor: NF1	99	99	0	6
UMHS-0032	41	F	I	R/Fr	CD	32	0	32	3
UMHS-0033	5	F	II	R/Ins	CD, gliosis	74	0	74	4
UMHS-0034	33	F	I	R/Fr	Gliosis	32	0	32	11
UMHS-0035	50	F	I	L/T	Gliosis	57	57	0	2
UMHS-0036	43	M	NR	L, R/T	CD/*Neuropace*	54	0	54	2
UMHS-0037	14	M	I	L/Fr	Tumor: DNET	50	0	50	—
UMHS-0038	28	M	II	L/T	MTS, gliosis	61	61	0	—
UMHS-0039	47	M	NR	R/P	CD/*Neuropace*	90	0	90	10
UMHS-0040	14	F	I	L/P	CD, gliosis	63	55	8	8
UMHS-0041	32	F	I	R/Fr	CD	71	0	71	9
UMHS-0043	28	M	II	R/T	Gliosis	86	0	86	9
UMHS-0044	45	F	NR	L/T, P	*Neuropace*	76	0	76	6
UMHS-0045	17	F	NR	L, R/T	*Neuropace*	94	0	94	15
UMHS-0046	23	F	I	L/Fr	CD	30	0	30	9
UMHS-0047	48	F	II	R/T	Gliosis	70	0	70	3
UMHS-0048	22	F	NR	L, R/T	*Neuropace*	86	0	86	8
UMHS-0049	53	F	NR	L, R/T	*Neuropace*	94	0	94	15
TOTALS/ averages						1985	793	1192	232

Abbreviations: CD, cortical dysplasia; DNET, dysembryoplastic neuroepithelial tumor; ECoG, electrocorticographic; F, female; Fr, frontal; HFO, high-frequency oscillation; ILAE, International League Against Epilepsy; Ins, insular; L, left; M, male; MTS, medial temporal sclerosis; NF1, neurofibromatosis type 1 tumor; NR, not resected; Occ, occipital; OUT, nonepileptic channels; P, parietal; PMG, polymicrogyria; PVNH, periventricular nodular heterotopia; R, right; SOZ, seizure onset zone channels; T, temporal; VNS, vagal nerve stimulator.

than simply an average over long epochs. We estimated HFO rates as a continuous function of time (cHFO rates), with the nonparametric Nelson-Aalen hazard rate model, and smoothed its output with kernel methods.[31–33] In a general sense, the Nelson-Aalen model gives the risk of an event's occurrence as a function of time, which is equivalent to its instantaneous rate.[32] This method has been used to quantify oscillatory activity during sleep[34] as well as the risk of seizures over time.[35]

Kernel smoothing methods can translate discrete events into continuous estimates of rate, but they require the selection of a bandwidth parameter, which generally controls how

Total recorded time, h	Total HFOs, n	Mean HFO rate, n/min/channel		HFO mean frequency, median, Hz		Recorded seizures, n		Responder subset membership		
		SOZ	OUT	SOZ	OUT	Total	Used	Mean rate	SOZ slope	OUT slope
168.8	400,123	1.99	0.17	156.2	161.6	5	1	X	X	
171.2	55,311	0.36	0.13	172.7	221.8	7	7			
179.5	459,037	1.91	0.47	169.9	166.8	9	6			
160.8	72,486	1.38	0.06	190.0	182.7	8	5		X	
164.3	354,931	0.83	0.34	157.0	166.4	20	9			
177.2	1,124,176	2.62	1.24	152.1	154.6	28	11			
207.7	269,638	1.77	0.88	161.6	172.8	10	3			X
246.2	390,187	1.52	0.51	165.3	166.3	40	7	X	X	X
205.2	1,212,921	2.98	2.19	148.3	154.0	97	8			X
79.7	198,968	2.39	0.37	154.3	159.2	7	4	X		
226.3	819,880	0.61	0.72	159.3	168.1	14	7			
146	378,824	1.01	0.56	152.3	169.0	33	12			
180	371,855	0.75	0.24	150.4	159.4	9	6			
184.3	382,400	2.45	0.64	159.4	170.5	8	6	X	X	X
120.7	150,963	0.97	0.30	169.8	219.7	28	19			
136.3	455,089	2.41	1.18	172.2	167.3	17	16			
162.7	122,451	0.67	0.19	147.9	172.4	7	6			
172.5	335,274	1.36	0.60	151.8	163.6	18	12			
219.7	229,207	—	0.30	—	157.3	34	22			
178.7	746,718	—	1.16	—	156.5	7	2			
155.2	233,050	0.99	0.22	160.6	184.0	19	7			
196.7	386,462	0.37	0.64	158.7	170.1	7	7			X
176.5	73,589	0.30	0.04	166.7	191.0	36	3			
182.2	279,124	0.75	0.33	170.9	226.8	46	5	X		
170.2	385,032	1.24	0.45	155.4	179.6	13	4			
331.5	645,420	0.76	0.24	167.3	185.8	6	6			
139.3	16,061	0.12	0.03	166.1	210.8	17	8			
301.7	417,307	0.65	0.22	155.0	196.8	1	1	X		
141.8	271,327	2.29	0.25	164.6	178.0	23	3	X		
176.8	179,259	0.63	0.11	179.6	166.9	17	4			
5459.5	11,417,070	1.29	0.49	162.0	178.1	591	217	7	4	5

jagged or smooth the estimate appears. We fixed this parameter at 1 minute for all patients, which prevented ictal HFOs from influencing preictal cHFO rates as the kernel window moved forward in time.

We computed cHFO rates with the Nelson-Aalen model in the same general manner as mean HFO rates, with one exception. Instead of using all interictal windows in the Nelson-Aalen computation, we restricted their number to be equal to the number of usable peri-ictal windows, choosing them at random from all usable interictal windows. While this allowed us to characterize interictal cHFO rates with the same temporal scale as peri-ictal cHFO rates, it

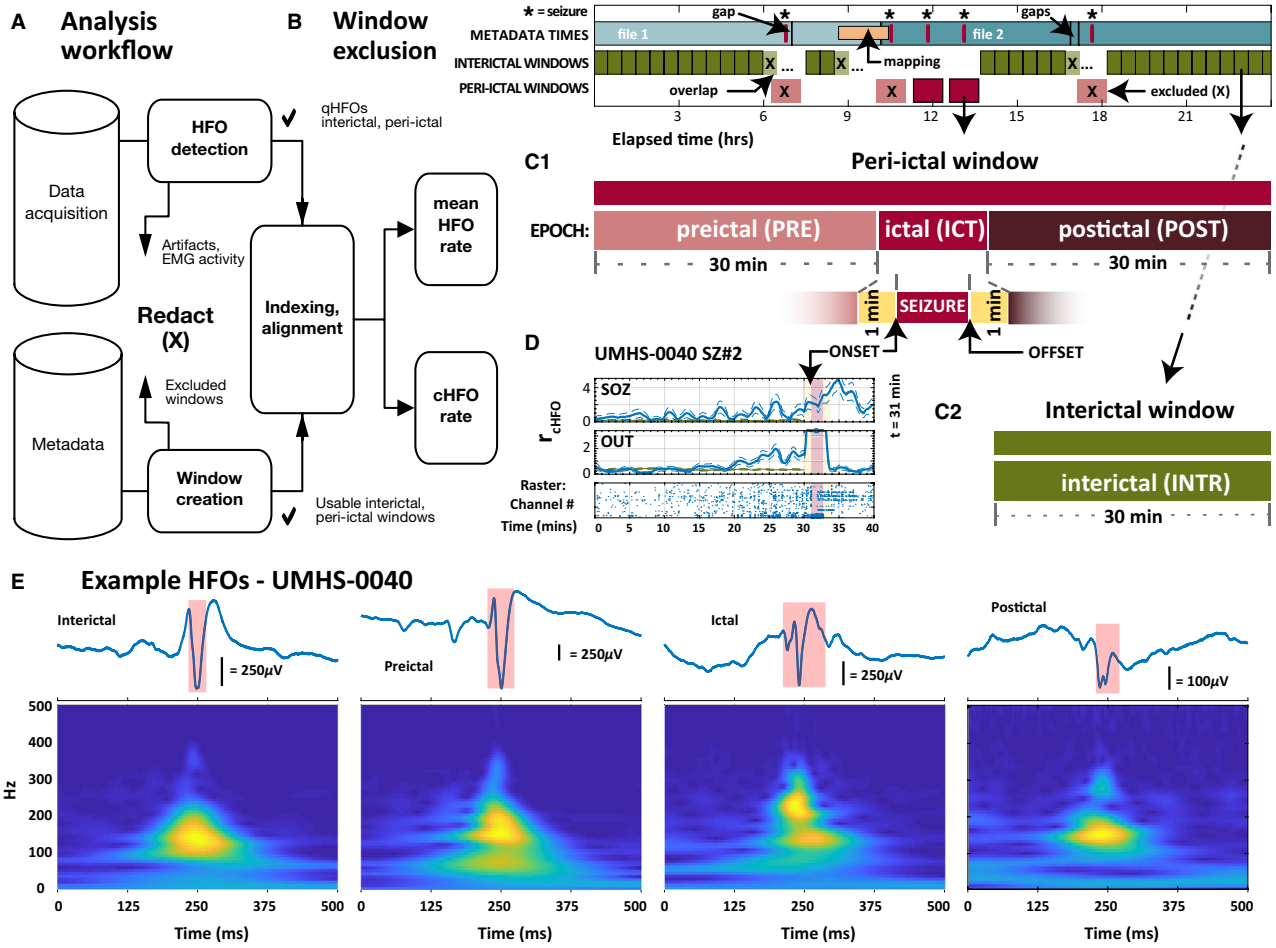

FIGURE 1 Schematic diagram showing overall data analysis workflow. A, Quality high-frequency oscillation (HFO) detections (quality HFOs [qHFOs]) and their respective interictal and peri-ictal windows of analysis are aligned in time to compute mean and continuous HFO rate. EMG, electromyographic. B, Analysis windows are created from patient metadata and excluded from further analysis if overlap occurs with a number of conditions that would bias results. C1, Remaining peri-ictal windows are further divided into preictal, ictal (which includes a 1-minute buffer on either side of the clinically marked seizure time), and postictal epochs. C2, Remaining interictal windows are defined as 30-minute epochs. D, Continuous HFO rate (cHFO) computed from a single seizure in an individual patient is shown for seizure onset zone channels (top row, SOZ) and nonepileptic channels (middle row, OUT). cHFO rates were computed from discrete HFO detections, shown as a raster plot of preictal detections (bottom row) and organized by channel index. This patient (UMHS-0040) was a member of the "slope responder" subset of patients and showed preictal increases in cHFO rate as onset approached. Here cHFO rate is defined as HFOs per minute per channel. Dotted lines indicate ±1 standard deviation; blue denotes preictal cHFO rate, and green denotes interictal cHFO rate for comparison. The peri-ictal window was truncated for display purposes at 40 minutes. E, Example HFO detections for the same patient in interictal, preictal, ictal, and postictal periods are visualized in time-frequency plots, each computed with the Morse wavelet

also meant that interictal cHFO rates were only calculated from a portion of the available data. To mitigate this, we repeated the calculation 10 times with different random selections and report the average of all 10 as the final estimate.

2.8 | Final analysis and statistical tests

After determining mean and continuous HFO rates for all patients, we compared interictal and peri-ictal rates across all patients. We assessed patientwise differences in mean HFO rate across channel groups (SOZ, OUT) and epochs (interictal, preictal) with the Wilcoxon signed rank test, using the appropriate Bonferroni correction. We also used the Kolmogorov-Smirnov test to compare differences in the population distributions of mean HFO rate across channel groups.

The cHFO rate is a continuous variable that estimates the instantaneous rate at every point in time. We first analyzed these results visually and noticed two clear groups of patients: (1) most patients had essentially stable cHFO rates preictally, which were similar to the interictal values; and (2) some patients had preictal cHFO rates that were larger than the interictal values and appeared to increase leading to the seizure. To quantify this difference, we fit a line to preictal and interictal cHFO trajectories using least

squares linear regression. We compared slopes of these lines within and across patients with the Wilcoxon signed rank test and further compared their overall distributions for different channel groups with the Kolmogorov-Smirnov test.

For both analyses, we used an unbiased, data-driven approach to identify natural clusters of outliers in the distributions by applying a kernel density estimator to the population distribution, then identifying local minima that distinguished any anomalous cluster, similar to our previous methods.[27] These minima were used as thresholds to identify putative responders.

2.9 | Data availability

HFO detection data and processing scripts used in this work are available from the authors upon request.

3 | RESULTS

Our automated HFO detector was run on the iEEG data of 30 patients (15 male, 15 female) from the University of Michigan health system. Patients in the study represented a diverse clinical cohort with a variety of ages, seizure foci, and epileptic etiologies. In total, >11.4 million HFOs from nearly 2,000 iEEG channels were detected and analyzed across >225 days of iEEG data. Further patient summary can be found in Table 1.

3.1 | Comparison of mean HFO rates

We first compared mean HFO rate across all the temporal epochs, an analysis that previously has been restricted almost exclusively to interictal periods. As shown in numerous prior studies, we found that SOZ channels had significantly higher mean rates than OUT channels for interictal and preictal epochs (Figure 2A, $P < .001$). Similar results occurred in ictal and postictal epochs (not shown, $P < .001$). We also compared mean HFO rates in different epochs across our population (not shown); ictal periods had much higher HFO rates than all other epochs (SOZ, OUT: $P < .001$), whereas postictal rates were quite variable among different patients but on average tended to be slightly higher than either interictal or preictal epochs, although this did not reach significance in all groups (data not shown).

The primary analysis was to compare inter- and preictal HFO rates. When averaged across all patients, there was no statistically significant difference in mean HFO rate between interictal and preictal epochs for either SOZ or OUT channel groups. In certain patients, however, we noticed that preictal rates were significantly higher than their interictal values, especially in the SOZ. This led to the possibility that specific patients might have large differences between inter- and preictal HFO rates that are not seen when averaged across all patients. We plotted the distribution among all patients of the difference between preictal and interictal rates for both channel groups. As shown in the histograms of Figure 2B, the distribution for OUT channels is centered at zero and is unimodal. In contrast, the distribution for SOZ channels appears

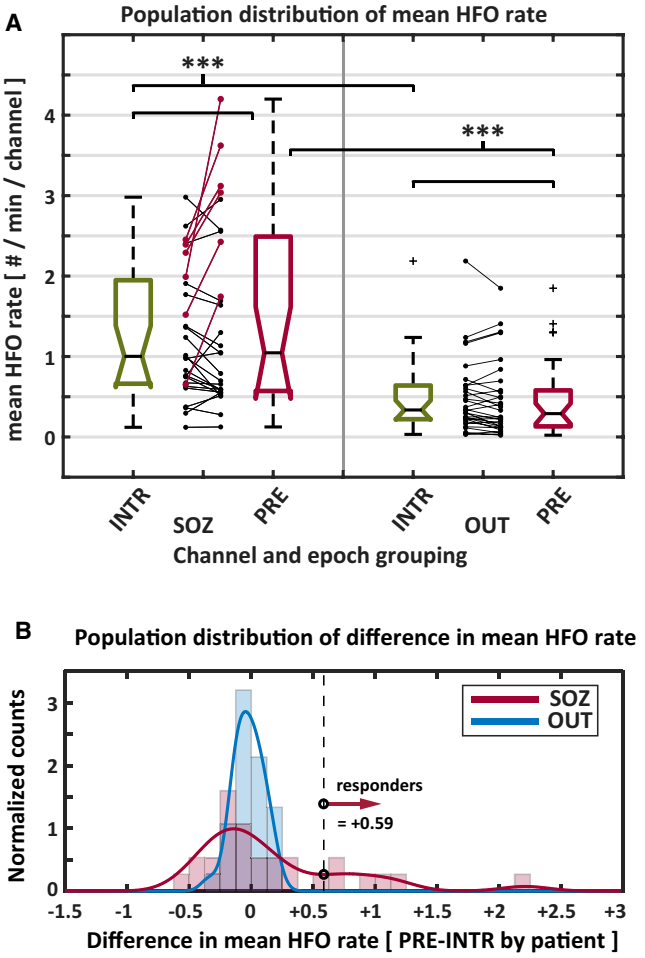

FIGURE 2 A, Population box plots of mean high-frequency oscillation (HFO) rate comparing interictal (INTR) and preictal (PRE) epochs, organized by channel group (seizure onset zone channels [SOZ], nonepileptic channels [OUT]). No statistical difference in mean HFO rate during interictal and preictal periods was found; mean rate in SOZ channels was significantly higher than OUT channels for all epochs (ictal and postictal, not shown: $P < .001$). Statistical comparisons performed (Wilcoxon signed rank test) are denoted by brackets at the top of each panel; asterisks show statistical significance, ***$P < .001$. Differences in raw data during interictal and preictal epochs are visualized per patient between box plot groups: "mean rate responders"—patients with increased difference in preictal rate in SOZ channels—are shown with red lines, whereas other patients are shown with black lines. B, Smoothed and binned population distributions of the difference in preictal versus interictal mean HFO rate are shown by channel group. OUT channels (blue) are unimodal, but SOZ channels are bimodal and show the presence of a "mean rate responder" patient subset (red), each having a difference in rate of 0.58 HFOs/min/channel

significantly skewed to the right, with several patients comprising the right tail of the distribution. This suggested that a distinct subset of "responder" patients in our cohort had significant increases in preictal HFO rates in the SOZ. Although these patients were too few to allow statistical tests to find strong independence of the SOZ and OUT distributions (Kolmogorov-Smirnov test, $P = .072$), they are clearly outliers in the SOZ distribution. The threshold to identify these outliers (first local minimum in the distribution of SOZ channels) was 0.58 HFOs/min/channel, yielding seven total "mean rate responders"—individuals for whom the difference in mean HFO rate for preictal and interictal epochs was much higher than the rest of the population. Patients who are within this subset are marked in Table 1 and labeled red in Figure 2A.

3.2 | Comparison of continuous HFO rates

We used the Nelson-Aalen hazard rate model to estimate HFO rate as a continuous function of time (cHFO rates). The result of this analysis for a single patient is shown in Figure 3, which superimposes the interictal and preictal cHFO rates for visual comparison. Calculating the cHFO rate creates a time-dependent function, which we evaluated mathematically (see next section). We first made visual observations of these functions, comparing the cHFO trajectories between interictal and preictal periods. As seen in Figure 3, this patient's preictal cHFO rate is generally higher than the interictal rate.

In our visual observations, we saw significant temporal variability in preictal cHFO trajectories within our patient cohort across channel groups and epochs. We identified patients with preictal cHFO trajectories that were similar to interictal ones (examples in Figure 4A). There were patients with increased preictal cHFO activity over interictal baseline (examples in Figure 4B,C); of these, some had distinct bursts of preictal cHFOs, and others had more sustained increases (Figure 4B). We also identified patients with preictal cHFO trajectories that appeared to increase gradually, leading to seizure onset (Figure 4C). These preictal trends were averaged across many seizures, but were also observed prior to individual seizures (Figure 4D). Even limited to visual inspection, these various changes were visible in at least 12 of the 30 patients. These example visual observations of preictal cHFO trends in various patients motivated further in-depth quantitative analysis, which we describe in detail below. Also, note that Figure 4 shows two patients (UMHS-0029 and -0040) in whom the HFO rate is higher in OUT compared with SOZ. As seen in Table 1, these were the only two patients who had this effect, which occurred when averaging over the entire region rather than selecting specific high-rate channels within the SOZ. Patient UMHS-0029 was not a responder, and UMHS-0040 had an atypical response described below.

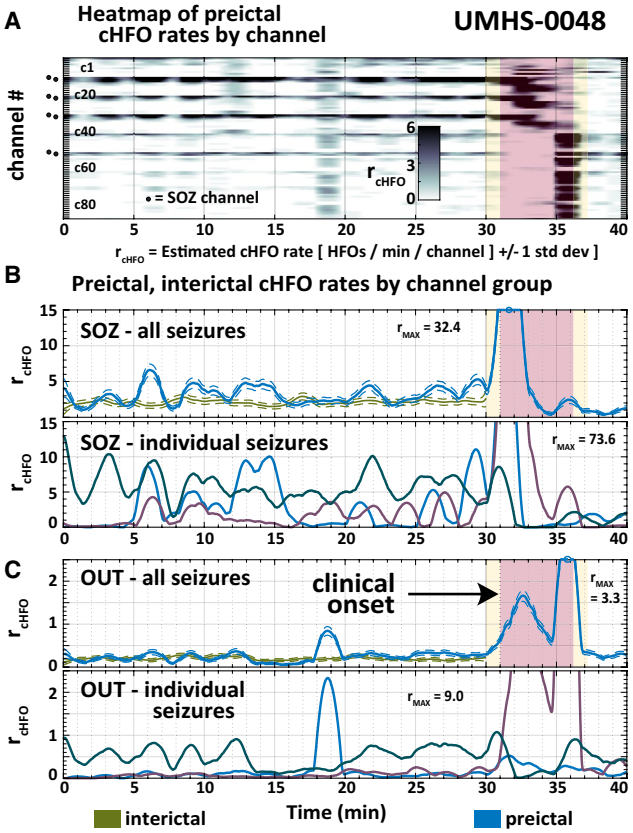

FIGURE 3 Example of continuous high-frequency oscillation (cHFO) rate analysis (Nelson-Aalen hazard rate estimate) for a single patient across multiple seizures, comparing preictal (blue) and interictal (green) epochs. This patient's preictal cHFO rates were on average higher than interictal rates. The scaled heatmap of cHFO rates (A) shows the contribution of individual channels to estimates computed from seizure onset zone channels (SOZ; B) and nonepileptic channels (OUT; C). Plots beneath B and C both show cHFO trajectories by individual seizure (without interictal reference). cHFO rate is defined as HFOs per minute per channel and is shown in the top rows of B and C with ±1 standard deviation (dotted lines). Yellow rectangles show the 1-minute ictal buffer, and red rectangles indicate the clinical duration of a given patient's longest seizure. The peri-ictal window was truncated for display purposes at 40 minutes

3.3 | Statistical significance of temporal trends

The visual observations in the previous section suggested that perhaps the change in the rate as seizures approach, rather than simply the magnitude, was associated with impending seizures. To quantify the temporal trends shown in Figure 4C, we compared the cHFO rates as mathematical functions. We used linear regression to fit a line to the 30-minute trajectory of cHFOs in the average preictal and interictal windows in each patient. These values are shown as population box plots in Figure 5A, where we define

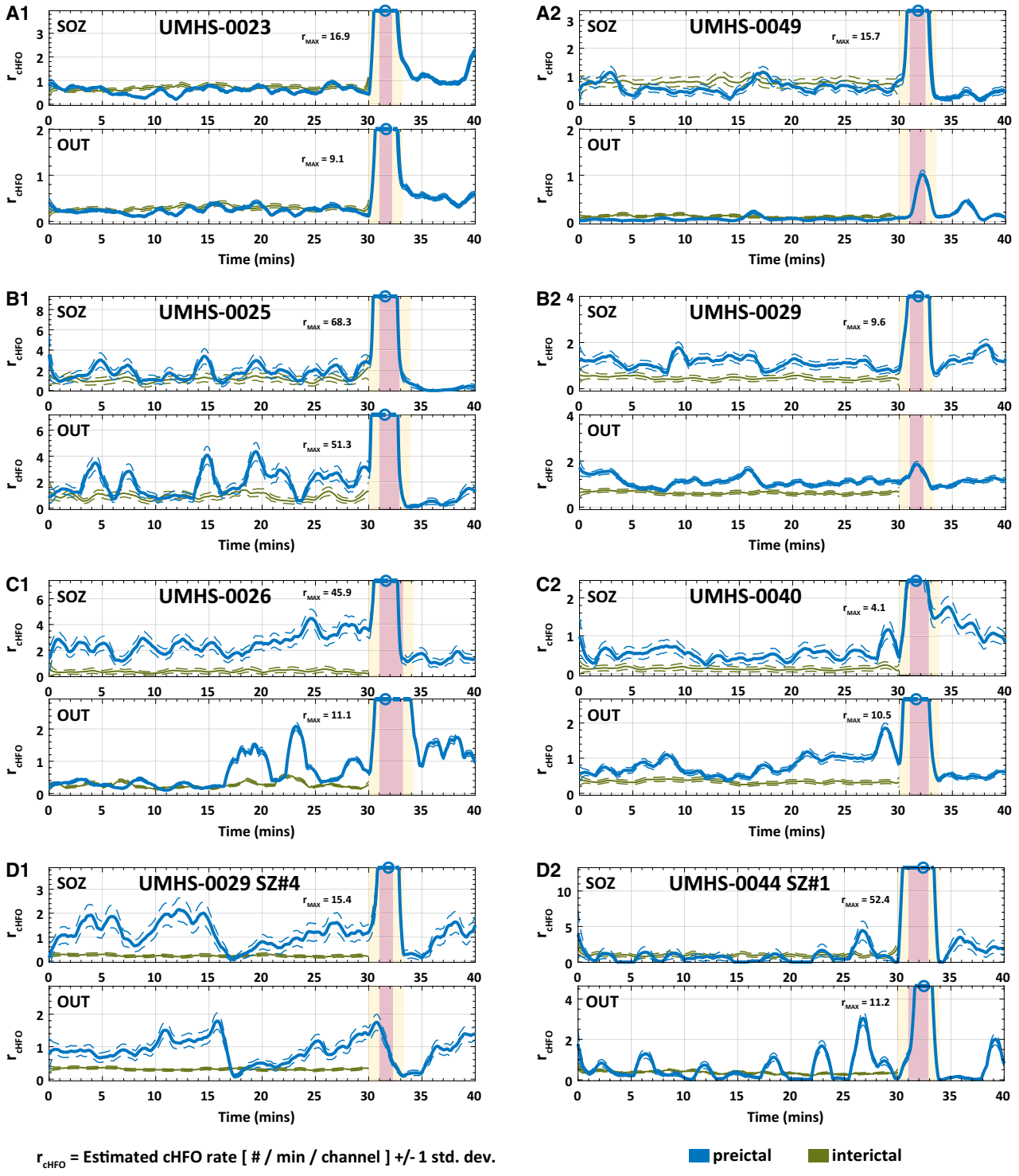

FIGURE 4 Variability of observed preictal continuous high-frequency oscillation (cHFO) rates. A, Many patients had few significant differences between interictal and preictal cHFO rates (example patients given in A1 and A2). B, Other patients displayed increased preictal cHFO trends relative to those of interictal periods; of these, periodic bursts of HFOs were evident in some (B1), whereas others showed more sustained increases in preictal HFO rates over interictal (B2). C, Two patients with gradually increasing preictal HFO rates were also identified. D, Examples of individual seizures in different patients, whose preictal cHFO rates also gradually increased toward onset, similarly to the average preictal trends of C. Here, cHFO rate is defined as HFOs per minute per channel. Visual formatting of all subfigures herein is the same as shown in Figure 3B,C. OUT, nonepileptic channels; SOZ, seizure onset zone channels; SZ, seizure

slope ($\Delta_{cHFO\ rate}$) as the change in HFO rate over 30 minutes, with rate given as HFOs per minute per channel. A number of patients had high preictal slope in SOZ channels, whereas across the population, interictal slopes were close to zero. We compared the distributions with a signed rank test, which takes pairwise differences between the preictal and interictal periods for each patient. The SOZ had a significant increase in slope (median$\Delta_{cHFO\ rate,\ PRE-INTR}$= 0.13, $P < .05$), whereas in OUT there was no appreciable difference (median$\Delta_{cHFO\ rate,\ PRE-INTR}$= 0.01, $P = .15$). As seen in Figure 5A, the differences were primarily due to certain patients with higher rate who were different from the rest of the group. To identify these potential outliers, we used a strategy similar to that shown in Figure 2B; we made a histogram of preictal slopes, fit them with a kernel density estimator, and looked for natural thresholds. In this case, the preictal distributions were statistically different from interictal ones for both channel groups (Kolmogorov-Smirnov: SOZ, OUT: $P < .05$, $P < .01$). The threshold for outliers, that is, "responders," was OUT$\Delta_{cHFO\ rate}$= +0.41, SOZ$\Delta_{cHFO\ rate}$ = +1.08. This gave a total of four patients in the "SOZ slope responder" subset, and five in the "OUT slope responder" subset (individuals marked in Table 1, and colored lines in Figure 5A). The responders were chosen solely on the basis of their preictal slopes being outliers, but note that the difference with interictal $\Delta_{cHFOrate,PRE-INTR}$ in each case was also very high. We thus conclude that the preictal change in cHFO rates is a novel potential biomarker of seizure onset.

3.4 | Relationship of responders with clinical metadata

We evaluated whether any of the three responder groups (mean rate, n = 7; SOZ rate, n = 4; OUT rate, n = 5) were correlated with clinical factors from Table 1. Of these responders, four had International League Against Epilepsy class I outcomes, four had class II, and three did not have resections (Table 1). We could not find any consistent demographical or etiological factor that was associated with a particular "responder" subset of patients; the rate of class I outcomes was similar to that of the whole group, and there were not enough patients to have sufficient power to identify specific differences in other factors such as location and pathology. We analyzed whether these results in 30 patients would be likely to apply to the larger epilepsy population. We evaluated this with a binomial confidence interval, with 30 samples and 11 successes ("responders"); the 95% confidence interval is 20%-56% (6-16 patients). Considering that as low as 38% of patients with refractory epilepsy achieve lasting seizure freedom after surgery,[36,37] we feel this responder rate is likely to have significant clinical impact as a biomarker. It is highly likely to be present in a large number of patients in larger studies.

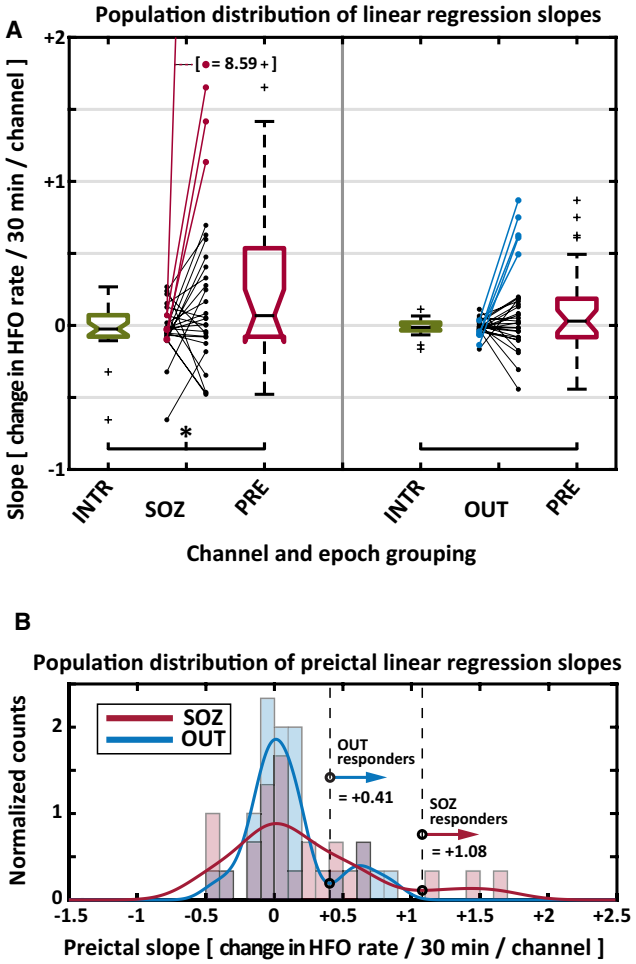

FIGURE 5 A, Population box plots of regression slopes fitted to continuous high-frequency oscillation (HFO) rates of interictal (INTR) and preictal (PRE) epochs, organized by channel group (seizure onset zone channels [SOZ], nonepileptic channels [OUT]). As a population, increased preictal slopes were observed only in SOZ channels (*$P < .05$, Wilcoxon signed rank test). Differences in raw data during interictal and preictal epochs are visualized per patient between box plot groups; "slope responders"—patients with increasing preictal continuous HFO (cHFO) rates in SOZ and OUT channels—are shown with red and blue lines respectively, whereas other patients are shown with black lines. B, Smoothed and binned population distributions of preictal cHFO regression slopes are shown by channel group; both SOZ and OUT distributions are bimodal. OUT slope responders (blue) have a slope threshold of +0.41 over 30 minutes, and SOZ slope responders (red) have a slope threshold of +1.08 over 30 minutes. Here, we define cHFO regression slope ($\Delta_{cHFOrate}$)as the change in HFO rate over 30 minutes, where HFO rate is defined previously as HFOs/minute/channel

4 | DISCUSSION

We performed a systematic analysis of time-varying HFO rates in a large cohort of patients with refractory epilepsy, robustly comparing interictal and peri-ictal rates for the first time. Our analysis of mean HFO rate found no

difference between preictal and interictal rates at a population level. Despite this, we used a data-driven approach to identify a putative subset of patients who are "mean rate responders," in whom there was a large difference between preictal and interictal rates. We also found that mean HFO rate was highest in SOZ channels, which corroborates existing findings that interictal HFOs localize epileptic tissue,[1,8,38] although we have confirmed it for preictal, ictal, and postictal epochs as well. Mean ictal HFO rates were significantly higher than rates for other epochs, a finding also supported in the literature.[23,39,40]

Prior HFO work has been based upon average rates over long windows (ie, 10 or 30 minutes). Here, we investigated peri-ictal HFO trends as a continuous function of time (cHFO rate), which estimates the "hazard rate" of HFOs occurring at any given moment in time. Despite little evidence of population-wide stereotypy, this revealed many varied and unique temporal patterns of peri-ictal cHFO trajectories among individuals. In our statistical analysis of cHFO rates, we compared the relative magnitude of preictal and interictal cHFO trends by their linear slope and again used their underlying distributions to identify two subsets of patients ("SOZ slope responders" and "OUT slope responders") with increased preictal cHFO activity relative to other patients.

These results are supported by previous findings, although there have been relatively few papers dealing with the effects of preictal HFOs. Early work found that HFOs had significant preictal changes in small cohorts of patients.[22,23] Other studies investigated high-frequency activity, but not necessarily discrete HFOs, and found similar results. One found that increases in 60-100 Hz power preceded seizure onset by as much 20 minutes in patients with refractory neocortical epilepsy.[10] Another showed that a predictive classifier of preictal state performed well in a subset of seven of 53 patients, each of whom showed distinct changes in preictal high-frequency activity that were coupled with slower brain rhythms.[41] The authors noted that their algorithm might have been successful in more patients if their cohort were more homogenous. Our work has quite similar results with HFOs; in our clinically diverse population, there were distinct subsets of patients in whom HFO rate reliably increased prior to seizures, albeit in different but complementary ways.

We did not identify any factors to predict which patients would be "responders"; however, it is important to point out that this is not a major concern, because the potential use case for HFOs as a temporal biomarker would require intracranial monitoring, which can be used to identify and train an algorithm post hoc. Thus, we do not anticipate that clinical metadata alone could be used to stratify which patients could be candidates. However, we did a deep analysis of the OUT slope responder group, as this indicated patients in whom HFO data suggested possible epileptic pathology outside of the SOZ. UMHS-0026 and -0032 were responders in all three groups, suggesting HFOs were strong biomarkers across all recorded channels. The other three, however, were only OUT slope responders. Two of them (UMHS-0025 and -0040) had secondary foci identified by the treating clinicians that were not included in the final SOZ channels. The other (UMHS-0027) had seizures with diffuse onsets. From this cohort, we hypothesize that high preictal change in HFO rate may be associated with the seizure-generating tissue, and may suggest an independent method of using HFOs to identify the epileptogenic zone. In other words, the OUT slope responders may indicate a previously unrecognized method to use HFOs to identify the epileptogenic zone.

This analysis has some clear limitations. HFO occurrence is not a linear phenomenon, so applying a linear regression to the rate cannot capture the complex brain dynamics that produce it, and we make no claim that it was the "best fit" to the data. This function was chosen as the simplest method to characterize a generic increase in HFO rate during the preictal period across patients. Our goal was to investigate gradual changes in preictal HFO rate across many seizures; accounting for nonlinear factors that would better model these variable cHFO trends was beyond the scope of this study. This analysis was designed to determine whether HFO rates were related to seizure onset, but was not designed to "predict seizures," as it averaged preictal behavior across many seizures. Furthermore, this work analyzed only the HFO rate; there are numerous additional features of the HFOs such as amplitude, spectral content, and duration[42] that will enrich this analysis in future work. There is also evidence of preictal EEG changes that may be applicable to HFOs,[19,23,43] and seizures themselves undergo changes in dynamical states, which may also affect HFOs. [44–46] These varied features provide a rich environment for future analyses, using robust methods to compare interictal and preictal data, to assess HFOs as a potential seizure prediction biomarker.[47,48]

4.1 | Conclusion

Our investigation found that peri-ictal HFO rates and trends vary significantly across patients and even within individuals. We found a subset of patients in whom HFOs could be a valuable tool to identify the preictal state. This potential biomarker could be utilized in future studies on seizure prediction, focusing on in-depth characterization of interictal variability of HFO rates and greater numbers of seizures. Additionally, such work could better define the role of pathologic high-frequency activity in the mechanisms of seizure generation and its implications for the disease of epilepsy as a whole.

ACKNOWLEDGMENTS

This study was supported by the National Institutes of Health (K01-ES026839 and R01-NS094399) and by the Robbins Family Research Fund and Lucas Family Research Fund at Michigan Medicine.

CONFLICT OF INTEREST

J.M.S. and S.R. have no conflicts of interest. W.C.S. and S.V.G. have a licensing agreement with Natus Medical but have received no financial remuneration.

ETHICAL PUBLICATION STATEMENT

We confirm that we have read the Journal's position on issues involved in ethical publication and affirm that this report is consistent with those guidelines.

ORCID

Jared M. Scott https://orcid.org/0000-0001-9656-916X
Stephen V. Gliske https://orcid.org/0000-0002-2259-2612
William C. Stacey https://orcid.org/0000-0002-8359-8057

REFERENCES

1. Jacobs J, Staba R, Asano E, Otsubo H, Wu JY, Zijlmans M, et al. High-frequency oscillations (HFOs) in clinical epilepsy. Prog Neurobiol. 2012;98:302–15.
2. Zijlmans M, Jiruska P, Zelmann R, Leijten F, Jefferys JGR, Gotman J. High frequency oscillations as a new biomarker in epilepsy. Ann Neurol. 2012;71:169–78.
3. Fujiwara H, Greiner HM, Lee KH, Holland-Bouley KD, Seo JH, Arthur T, et al. Resection of ictal high-frequency oscillations leads to favorable surgical outcome in pediatric epilepsy. Epilepsia. 2012;53:1607–17.
4. Haegelen C, Perucca P, Châtillon CE, Andrade-Valença L, Zelmann R, Jacobs J, et al. High-frequency oscillations, extent of surgical resection, and surgical outcome in drug-resistant focal epilepsy. Epilepsia. 2013;54:848–57.
5. Cho JR, Koo DL, Joo EY, Seo DW, Hong SC, Jiruska P, et al. Resection of individually identified high-rate high-frequency oscillations region is associated with favorable outcome in neocortical epilepsy. Epilepsia. 2014;55:1872–83.
6. Höller Y, Kutil R, Klaffenböck L, Thomschewski A, Höller PM, Bathke AC, et al. High-frequency oscillations in epilepsy and surgical outcome. A meta-analysis. Front Hum Neurosci. 2015;9:1–14.
7. Fedele T, Burnos S, Boran E, Krayenbühl N, Hilfiker P, Grunwald T, et al. Resection of high frequency oscillations predicts seizure outcome in the individual patient. Sci Rep. 2017;7:1–10.
8. Frauscher B, Bartolomei F, Kobayashi K, Cimbalnik J, van 't Klooster MA, Rampp S, et al. High-frequency oscillations: the state of clinical research. Epilepsia. 2017;58:1316–29.
9. Dzhala VI, Staley KJ. Transition from interictal to ictal activity in limbic networks in vitro. J Neurosci. 2003;23:1–8.
10. Worrell GA, Parish L, Cranstoun SD, Jonas R, Baltuch G, Litt B. High-frequency oscillations and seizure generation in neocortical epilepsy. Brain. 2004;127:1496–506.
11. Jiruska P, Csicsvari J, Powell AD, Fox JE, Chang WC, Vreugdenhil M, et al. High-frequency network activity, global increase in neuronal activity, and synchrony expansion precede epileptic seizures in vitro. J Neurosci. 2010;30:5690–701.
12. Sato Y, Doesburg SM, Wong SM, Boelman C, Ochi A, Otsubo H. Preictal surrender of post-spike slow waves to spike-related high-frequency oscillations (80–200 Hz) is associated with seizure initiation. Epilepsia. 2014;55:1399–405.
13. Malinowska U, Bergey GK, Harezlak J, Jouny CC. Identification of seizure onset zone and preictal state based on characteristics of high frequency oscillations. Clin Neurophysiol. 2015;126:1505–13.
14. Salami P, Lévesque M, Avoli M. High frequency oscillations can pinpoint seizures progressing to status epilepticus. Exp Neurol. 2016;280:24–9.
15. Levesque M, Salami P, Gotman J, Avoli M. Two seizure-onset types reveal specific patterns of high-frequency oscillations in a model of temporal lobe epilepsy. J Neurosci. 2012;32:13264–72.
16. Bragin A, Wilson CL, Almajano J, Mody I, Engel J. High-frequency oscillations after status epilepticus: epileptogenesis and seizure genesis. Epilepsia. 2004;45:1017–23.
17. Traub RD, Whittington MA, Buhl EH, LeBeau FEN, Bibbig A, Boyd S, et al. A possible role for gap junctions in generation of very fast EEG oscillations preceding the onset of, and perhaps initiating, seizures. Epilepsia. 2001;42:153–70.
18. Jiruska P, Alvarado-Rojas C, Schevon CA, Staba R, Stacey W, Wendling F, et al. Update on the mechanisms and roles of high-frequency oscillations in seizures and epileptic disorders. Epilepsia. 2017;58:1330–9.
19. Stacey W, Le Van QM, Mormann F, Schulze-Bonhage A. What is the present-day EEG evidence for a preictal state? Epilepsy Res. 2011;97:243–51.
20. Litt B, Esteller R, Echauz J, D'Alessandro M, Shor R, Henry T, et al. Epileptic seizures may begin hours in advance of clinical onset: a report of five patients. Neuron. 2001;30:51–64.
21. Mormann F, Kreuz T, Rieke C, Andrzejak RG, Kraskov A, David P, et al. On the predictability of epileptic seizures. Clin Neurophysiol. 2005;116:569–87.
22. Jacobs J, Zelmann R, Jirsch J, Chander R, Châtillon CE, Dubeau F, et al. High frequency oscillations (80–500 Hz) in the preictal period in patients with focal seizures. Epilepsia. 2009;50:1780–92.
23. Pearce A, Wulsin D, Blanco JA, Krieger A, Litt B, Stacey WC. Temporal changes of neocortical high-frequency oscillations in epilepsy. J Neurophysiol. 2013;110:1167–79.
24. Blanco JA, Stead M, Krieger A, Stacey W, Maus D, Marsh E, et al. Data mining neocortical high-frequency oscillations in epilepsy and controls. Brain. 2011;134:2948–59.
25. Matsumoto A, Brinkmann BH, Stead SM, Matsumoto J, Kucewicz MT, Marsh WR, et al. Pathological and physiological high-frequency oscillations in focal human epilepsy. J Neurophysiol. 2013;110:1958–64.
26. Ren S, Gliske SV, Brang D, Stacey WC. Redaction of false high frequency oscillations due to muscle artifact improves specificity to epileptic tissue. Clin Neurophysiol. 2019;130:976–85.
27. Gliske SV, Irwin ZT, Davis KA, Sahaya K, Chestek C, Stacey WC. Universal automated high frequency oscillation detector for real-time, long term EEG. Clin Neurophysiol. 2016;127:1057–66.
28. Staba RJ, Wilson CL, Bragin A, Fried I, Engel J. Quantitative analysis of high-frequency oscillations (80–500 Hz) recorded in human

epileptic hippocampus and entorhinal cortex. J Neurophysiol. 2002;88:1743–52.
29. Abend NS, Gutierrez-Colina A, Marsh E, Clancy RR, Dlugos DJ, Zhao H, et al. Interobserver reproducibility of EEG interpretation in critically ill children. J Clin Neurophysiol. 2011;28:333–4.
30. Benbadis SR, Lafrance WC, Papandonatos GD, Korabathina K, Lin K, Kraemer HC. Interrater reliability of EEG-video monitoring. Neurology. 2009;73:843–6.
31. Aalen O. Nonparametric inference for a family of counting processes. Ann Stat. 2007;6:701–26.
32. Muller H-G, Wang J-L. Hazard rate estimation under random censoring with varying kernels and bandwidths. Biometrics. 1994;50:61–76.
33. Muller H-G, Stadtmuller U. Variable bandwidth kernel estimators of regression curves. Ann Stat. 1987;15:182–201.
34. Sedigh-Sarvestani M, Thuku GI, Sunderam S, Parkar A, Weinstein SL, Schiff SJ, et al. Rapid eye movement sleep and hippocampal theta oscillations precede seizure onset in the tetanus toxin model of temporal lobe epilepsy. J Neurosci. 2014;34:1105–14.
35. Luna-Munguia H, Starski P, Chen W, Gliske S, Stacey WC. Control of in vivo ictogenesis via endogenous synaptic pathways. Sci Rep. 2017;7:1–13.
36. Wiebe S, Blume WT, Girvin JP, Eliasziw M. A randomized, controlled trial of surgery for temporal-lobe epilepsy. N Engl J Med. 2001;345:311–8.
37. Noe K, Sulc V, Wong-Kisiel L, Wirrell E, Van Gompel JJ, Wetjen N, et al. Long-term outcomes after nonlesional extratemporal lobe epilepsy surgery. JAMA Neurol. 2013;70:1003–8.
38. Andrade-Valença L, Mari F, Jacobs J, Zijlmans M, Olivier A, Gotman J, et al. Interictal high frequency oscillations (HFOs) in patients with focal epilepsy and normal MRI. Clin Neurophysiol. 2012;123:100–5.
39. Zijlmans M, Jacobs J, Kahn YU, Zelmann R, Dubeau F, Gotman J. Ictal and interictal high frequency oscillations in patients with focal epilepsy. Clin Neurophysiol. 2011;122:664–71.
40. Modur PN, Zhang S, Vitaz TW. Ictal high-frequency oscillations in neocortical epilepsy: implications for seizure localization and surgical resection. Epilepsia. 2011;52:1792–801.
41. Alvarado-Rojas C, Valderrama M, Fouad-Ahmed A, Feldwisch-Drentrup H, Ihle M, Teixeira CA, et al. Slow modulations of high-frequency activity (40–140 Hz) discriminate preictal changes in human focal epilepsy. Sci Rep. 2014;4:1–9.
42. Bragin A, Azizyan A, Almajano J, Wilson CL, Engel J. Analysis of chronic seizure onsets after intrahippocampal kainic acid injection in freely moving rats. Epilepsia. 2005;46:1592–8.
43. Baud MO, Kleen JK, Mirro EA, Andrechak JC, King-Stephens D, Chang EF, et al. Multi-day rhythms modulate seizure risk in epilepsy. Nat Commun. 2018;9:1–10.
44. Jirsa VK, Stacey WC, Quilichini PP, Ivanov AI, Bernard C. On the nature of seizure dynamics. Brain. 2014;137:2210–30.
45. Lopes da Silva FH, Blanes W, Parra J, Velis DN, Kalitzin SN, Suffczynski P. Dynamical diseases of brain systems: different routes to epileptic seizures. IEEE Trans Biomed Eng. 2003;50:540–8.
46. Saggio ML, Crisp D, Scott J, Karoly PJ, Kuhlmann L, Nakatani M, et al. A taxonomy of seizure dynamotypes. Elife. 2020;9:e55632.
47. Snyder DE, Echauz J, Grimes DB, Litt B. The statistics of a practical seizure warning system. J Neural Eng. 2008;5:392–401.
48. Mormann F, Andrzejak RG, Elger CE, Lehnertz K. Seizure prediction: the long and winding road. Brain. 2007;130:314–33.

How to cite this article: Scott J, Ren S, Gliske S, Stacey W. Preictal variability of high-frequency oscillation rates in refractory epilepsy. *Epilepsia*. 2020;61:2521–2533. https://doi.org/10.1111/epi.16680